

Silver-reduced Graphene Oxide Composites prepared by spin coating technique as Cathode Material for Dye-Sensitized Solar Cells

M.Y.A. Rahman*, N. Mustaffa

Institute of Microengineering and Nanoelectronics (IMEN), Universiti Kebangsaan Malaysia, 43600, Bangi, Selangor, Malaysia

*E-mail: mohd.yusri@ukm.edu.my

Received: 14 January 2021 / Accepted: 4 March 2021 / Published: 30 April 2021

Silver-reduced graphene oxide (Ag-rGO) composite films have been prepared via layer-by-layer spin coating method. The Ag-rGO samples were then employed as cathode in a dye-sensitized solar cell (DSSC). The main aim of this work is to study the relationship between spin coating cycle of Ag-rGO with the performance parameters of the device. Various spin coating cycles have been chosen, namely, 3,4,5,6 and 7 times. The highest transmittance of the sample is 7.5% corresponding with 3 spin-coating cycles. The highest η of 0.840%, J_{sc} of 4.404 mA cm⁻² and FF of 0.329 were obtained from the device with 4 spin-coating cycles. This is due to this device has the smallest charge transfer resistance at the interface of Ag-rGO/electrolyte (R_{ct1}) of 14.37 Ω .

Keywords: cathode; dye-sensitized solar cells; reduced graphene oxide; silver

1. INTRODUCTION

Platinum (Pt) film is a popular material as cathode in dye-sensitized solar cell (DSSC) since it is the most stable material against corrosion caused by redox mediator such as iodide/triiodide and sulfide/polysulfide. Furthermore, it possesses good electronic conductivity to accept electrons from external circuit. It also has high catalytic activity for fast reduction of triiodide to iodide. However, the use of Pt as cathode for the device in large scale is impractical since its price is very expensive. Therefore, several research groups have attempted alternative materials to replace Pt as cathode in DSSC [1-8]. Some groups have utilized carbon based materials due to its low resistance and high catalytic activity [3,4,9]. Reduced graphene oxide (rGO) is also popular material as free-Pt cathode producing comparable power conversion efficiency to that of Pt based device since it also possesses high conductivity and

catalytic activity [9-12]. rGO was attempted as cathode for the device but produced low efficiency that was 0.09% [13].

In order to further increase the efficiency, gold was doped into rGO and Au-rGO sample was then employed as cathode for the device. As a result, the efficiency was slightly improved to 0.175% [14]. Doping gold into rGO was found as an effective way of improving the electronic conductivity of rGO and consequently improved the efficiency of the device. Phosphorous doped rGO cathode produced the highest efficiency of 6.04% at 1.27 percentage by atomic of phosphorous [15]. In 2016, it has been reported that silicon doped rGO cathode yielded the efficiency of 4.94% [16]. While, the DSSC utilized nitrogen doped rGO cathode achieved the efficiency of 4.26% [17].

In this work, we have prepared Ag-rGO films composites and employed as cathode for the device. Ag has been chosen as it is expected to improve the electronic conductivity of rGO when it is prepared in composite form. The new idea of this work is the use of Ag-rGO films as cathode for the device. The goal of this work is to correlate the preparation parameter of Ag-rGO that is spin coating cycle with its optical transmission and the photovoltaic parameters of the device.

2. METHODOLOGY

At first, GO sheet was synthesized via modified Hummer's method, following the procedures described in [18]. 0.1 g GO sheet was then dissolved in 10 ml deionized water and stirred ultrasonically for 1 h. 0.05 M AgNO_3 M was put into 5 ml deionized water and the solution was then added to the GO solution. The mixture solution was stirred ultrasonically for another 3 hrs and 30 mins. The solution was then deposited on ITO substrate by spin coating technique at 1550 rpm for 30 s for preparation of Ag-GO film. This procedure was repeated 3 times in order to obtain the films with sufficient thickness. Ag-GO sample was then underwent annealing treatment at 350 °C in nitrogen environment for 1 hr in to reduce Ag-GO to Ag-rGO film. Ag-rGO samples with other spin coating cycles, namely, 4, 5, 6 and 7 were prepared by repeating these procedures. The transmittance of the samples was studied by UV-Vis spectrometer. The phase structure of the sample prepared at 3 spin-coating cycles was determined by XRD. The morphology of the sample was characterized by FESEM. The elemental composition analysis of the sample was performed by EDX.

The TiO_2 films prepared by liquid phase deposition technique was utilized as a photoanode of the device. The procedures of preparing the films via this technique is described in [19]. 0.3959 g ammonium heksaflorotitanat (AHT) with the concentration of 0.1 M and 0.2474 g boric acid with the concentration of 0.2 M have been dissolved in 20 ml of deionized water, respectively. Each of 5 ml of both solutions was mixed. ITO substrate was then vertically immersed in the mixed solution and heated at 50 °C for 5 hours in a furnace. Then, the substrate that has been coated with TiO_2 was rinsed with deionized water to remove the impurities that resides on the sample. Finally, the sample was annealed at 400 °C for 1 hour in a furnace to improve the adhesion of TiO_2 on ITO substrate.

The N719 dye powder was dissolved into ethanol. The TiO_2 films were then coated in 5 mM N719 dye in order to improve its optical absorption in visible region of light spectrum. The immersion of TiO_2 into N719 solution was carried out for 15 h at room temperature. The active area of the device

for light illumination was 0.23 cm^2 . The prepared Ag-rGO composite was used a cathode of the device. The performance study of the device was carried out by observing current-voltage curve in dark and under illumination of 100 mW cm^{-2} light from tungsten halogen lamp. For each spin coating cycle, five devices have been fabricated and tested. The electrochemical impedance spectroscopy (EIS) parameters such as series resistance (R_s), charge transfer resistance (R_{ct}) and carrier life time (τ) were obtained by conducting electrochemical impedance spectroscopy (EIS) measurement under illumination with the same intensity as that of performance study.

3. RESULTS AND DISCUSSION

Fig. 1 depicts the XRD pattern of Ag-rGO sample prepared with 3 spin-coating cycles. The sample contains 2 phases, namely, rGO and Ag. The XRD pattern shows a broad peak that belongs to rGO at the diffraction angle (2θ)= 24.0° with the interlayer d -spacing of 0.37 nm. This is a typical pattern of amorphous carbon structure, revealing the formation of rGO. The peaks at 31, 36, 51 and 61° belong to ITO substrate. Silver peaks appear at $2\theta = 38, 44, 64,$ and 77° corresponding with the crystallographic planes of (111), (200), (220), and (311), of the face-centered cubic of Ag, respectively, according to the International Centre for Diffraction Data (ICDD).

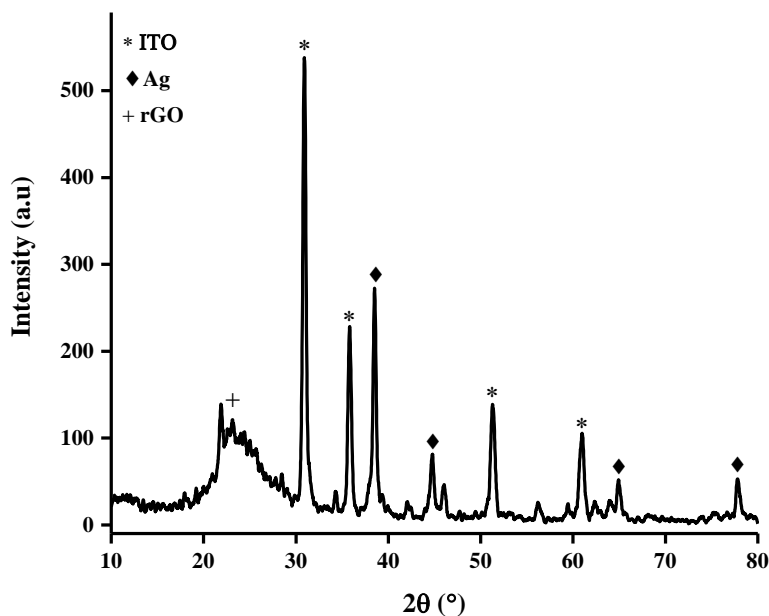


Figure 1. XRD pattern of Ag-rGO composite [20]

Fig. 2 shows the FESEM micrographs of the Ag-rGO sample prepared at 3 spin-coating cycles with 5000 and 30,000 \times magnifications, respectively. The images show the dark region and white strips. The white strips belong to rGO. It is observed that white silver particles reside on the surface of rGO since they do not occupy the site of rGO lattice. At 30,000 \times magnifications, the white strips and white particles are clearer to be seen.

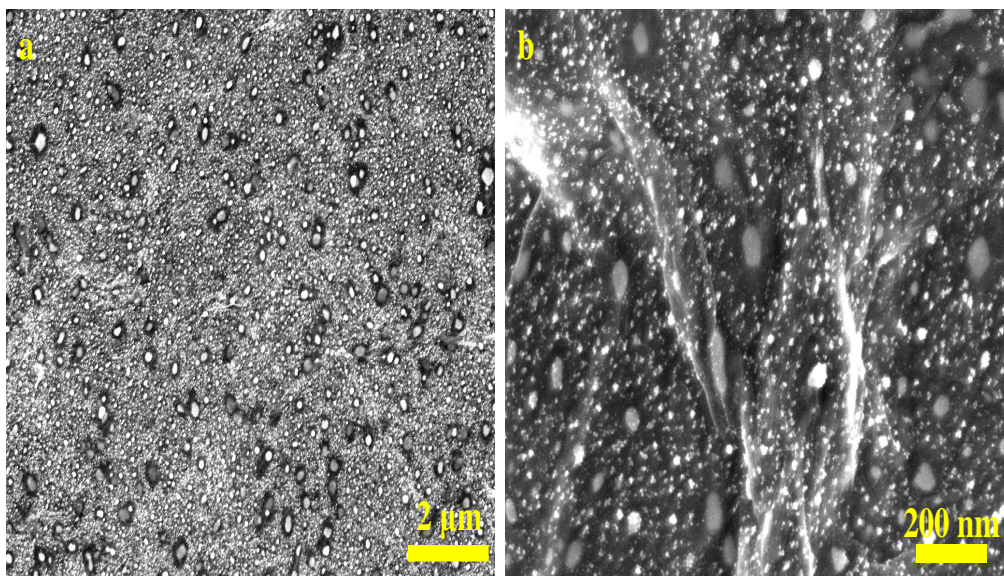


Figure 2. FESEM image of Ag-rGO composite (a), 5000× and b) 30000× magnifications [20]

Fig. 3 shows the EDX spectrum of the sample prepared at 3 spin-coating cycles. The EDX spectrum shows the composition percentage of each element that exists in Ag-rGO sample. The weight percent of carbon, oxygen and argentum is 53.1, 25.9 and Ag 21.0%, respectively. Carbon and oxygen elements originate from rGO. The weight percent of oxygen is found to be smaller than that of carbon and oxygen.

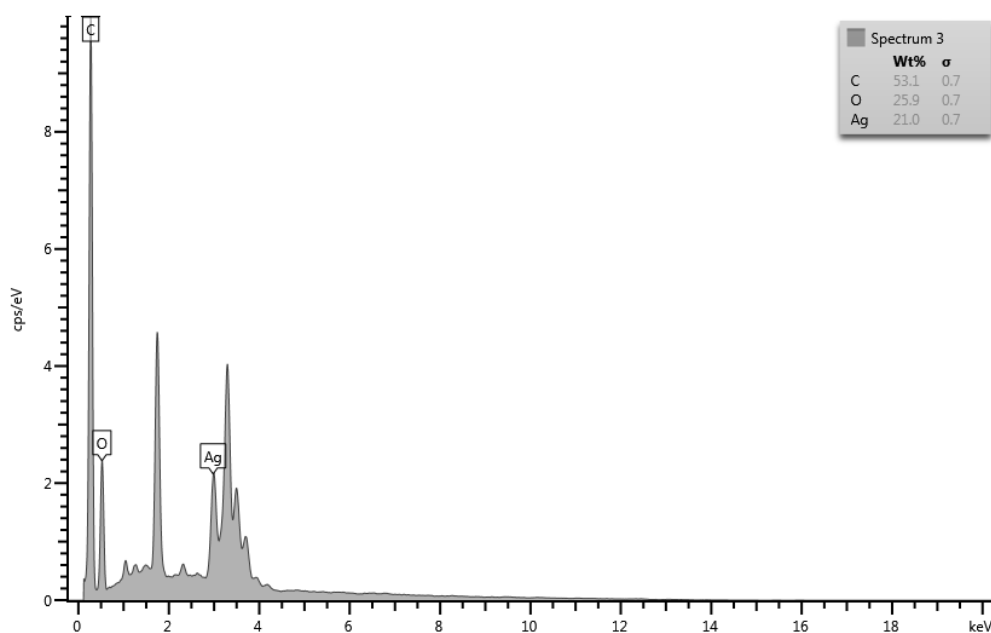


Figure 3. EDX spectrum of Ag-rGO sample

Fig. 4 depicts the optical transmission spectra of Ag-rGO samples with various spin coating cycles in the wavelength region 300-800 nm. According to the spectra, the optical transmittance decreases with the increase of spin coating cycle. The sample with 3 spin-coating cycles possesses the highest transmittance of 7.5% while that with 6 spin-coating cycles owns the lowest transmittance around 0.3% in the visible region. The decrease in transmittance with the spin coating cycle is due to the increase in thickness of the samples. As well understood, the thickness of the sample increases as spin coating cycle is increased. Thicker films transmit less amount of light compared with thinner films. It is also observed from Fig. 4 that the sample with 3 and 4 spin-coating cycles own higher transmittance in visible region (400-800 nm) than that in UV region (300-400 nm).

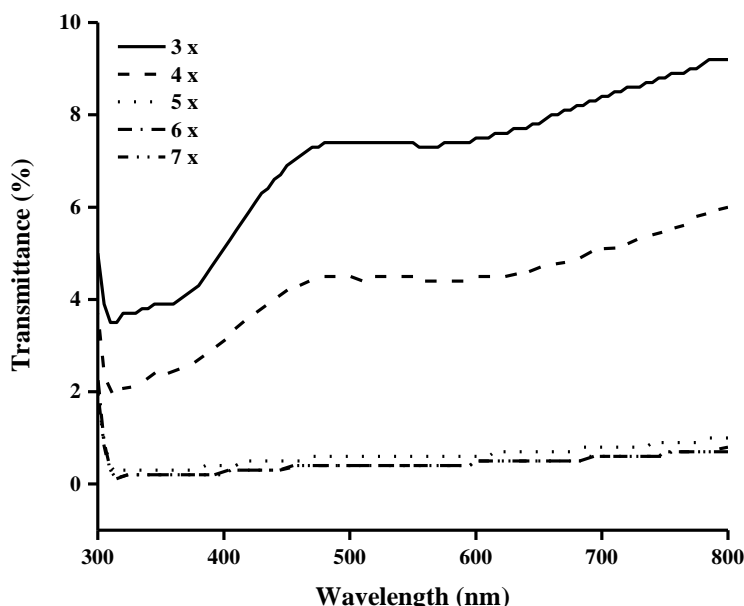


Figure 4. UV-VIS transmission spectra of Ag-rGO counter electrode with various spin coating cycles

Fig. 5 illustrates the dark current curves of the device using Ag-rGO films cathode with various spin coating cycles. It is noticed that the leak current which is the current in reverse bias is larger than forward bias current for all devices. Higher leak current causes lower output power generated in the device as illustrated in Fig. 6. According to Fig. 5, it is found that the spin coating cycle influences the dark current. The device with 3 spin-coating cycles has the lowest leak current and the one with 4 spin-coating cycles owns the largest leak current. The device with 4 spin-coating cycles has the largest forward current and the one with 6 spin-coating cycles possesses the lowest forward current.

Fig. 6 depicts the J - V curves of the device with various spin coating cycles. It is found that the shape of the J - V curves for the devices utilizing Ag-rGO cathode with various spin coating cycles do not follow the shape of the typical J - V curves [21-25]. The slope for all curves are high signifying high internal resistance in the devices. The photovoltaic parameters are extracted from Fig. 6 and illustrated in Table 1. According to Table 1, it is observed that the device with 4 spin-coating cycles performs the highest photovoltaic parameters except V_{OC} . This is because this device has the smallest R_{ct} as shown in Table 2. The DSSC with 3 spin-coating cycles performs the lowest these photovoltaic parameters due to

the shortest τ as listed in Table 2. The charge carriers are transported faster within the device with lower bulk resistance. The longer carrier life time, the slower electrons recombine with holes, thus causing the increase in the photocurrent and consequently the efficiency of the device. Also, according to the table, it is seen that the V_{OC} is not significantly influenced by spin coating cycle.

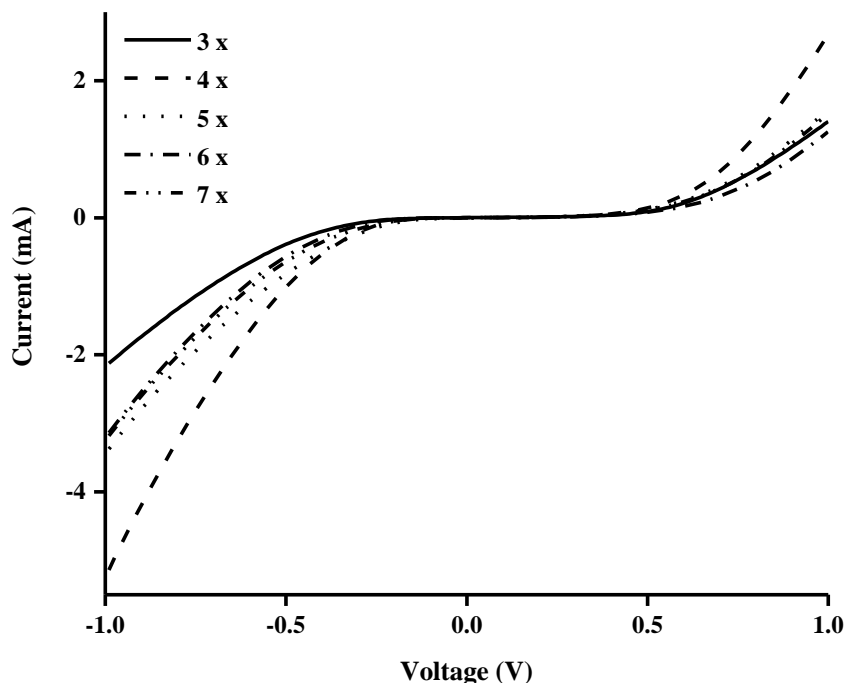


Figure 5. *I-V* curves with different spin coating layers

According to Table 1, the highest η that is 0.840% is found to be smaller than that reported in [11] that was 6.04%. This is due to its charge transfer resistance is higher than that reported in [11]. However, it is higher than that reported in [10] that was 0.175%. This is because the charge transfer resistance at the interface of Ag-rGO/electrolyte that is 14.4Ω is smaller than that of the device utilizing Au-rGO that was 69.0Ω [10]. It is also slightly higher than that of the device fabricated in our previous work concerning with the scope of variation of AgNO_3 concentration that was 0.746% [26]. Nevertheless, it is lower than that in the scope of annealing temperature that was 1.30% [20]. This is due to the resistance at the interface of $\text{TiO}_2/\text{N719}/\text{electrolyte}$ of this work is lower than that reported in [26]. This is also caused by the resistance at the interface of Ag-rGO of this work is higher than that reported in [20]. Also, the highest η obtained from this work is lower than that of the device utilizing NiS-rGO and NiPd-rGO cathodes corresponding with the η of 1.04 and 2.13%, respectively [27,28].

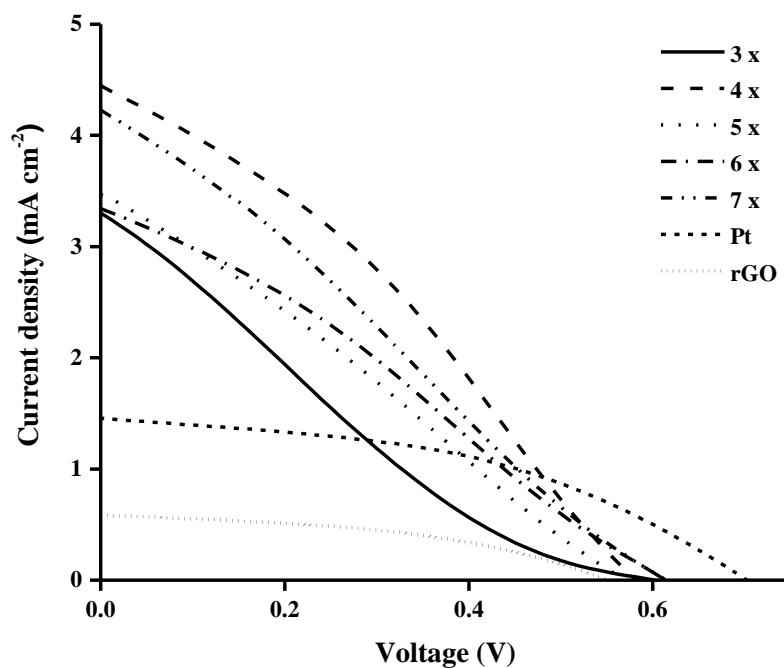


Figure 6. *J-V* curves under illumination with various spin coating cycles

Table 1. Photovoltaic parameters with various spin coating cycles

Sample	J_{SC} (mA cm ⁻²)	V_{OC} (V)	η (%)	FF
rGO	0.543 ± 0.022	0.540 ± 0.006	0.136 ± 0.002	0.466 ± 0.016
Pt	1.456	0.699	0.453	0.444
3	3.250 ± 0.202	0.590 ± 0.003	0.392 ± 0.023	0.204 ± 0.005
4	4.404 ± 0.096	0.580 ± 0.006	0.840 ± 0.030	0.329 ± 0.002
5	3.441 ± 0.151	0.530 ± 0.009	0.537 ± 0.035	0.294 ± 0.003
6	3.309 ± 0.120	0.610 ± 0.003	0.595 ± 0.026	0.295 ± 0.001
7	4.177 ± 0.159	0.600 ± 0.012	0.686 ± 0.039	0.265 ± 0.001

Fig. 7 and 8 illustrate the Nyquist and Bode curves of the device with various spin coating cycles. The series resistance (R_b) and charge transfer resistance at the interface of Ag-rGO/electrolyte (R_{ct}) are estimated from Fig. 7 and presented in Table 2. The straight line from 0Ω along $-Z$ -axis to the starting point of first semi-curve represents R_b . While, R_{ct} is denoted by the diameter of first semi-curve. The charge carrier lifetime is determined from Fig. 8 and also listed in Table 2. According to the table, it is found that R_b is not significantly influenced by spin coating cycle as their value does not much differ. Also, R_{ct} is found to neither show the increasing or decreasing trend with spin coating cycle. The device with 4 spin-coating cycles possesses the lowest R_{ct} . While, the device with 6 spin-coating cycles owns the highest R_{ct} . The device using Ag-rGO sample prepared at 7 spin-coating cycles exhibits the longest lifetime whereas the one that employs the sample prepared at 3 and 5 spin-coating cycles shares the

shortest lifetime. Also, it is said that the spin coating cycle does not affect the carrier lifetime as it is in the small range 20-25 ms corresponding with 3-7 spin-coating cycles.

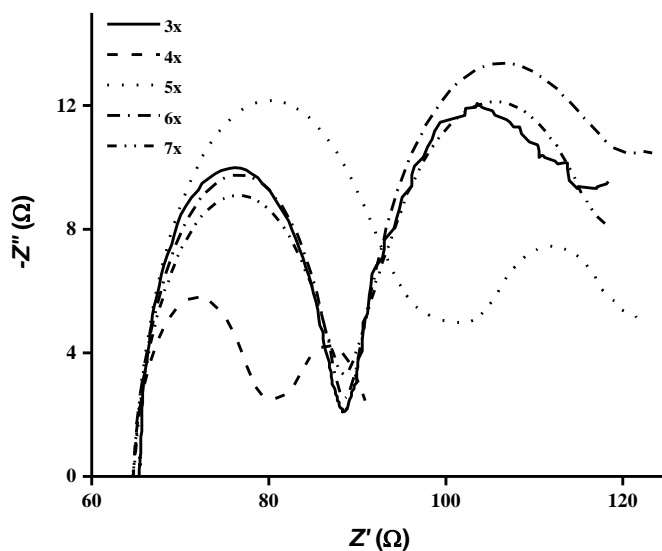


Figure 7. Nyquist plots with various spin coating cycles

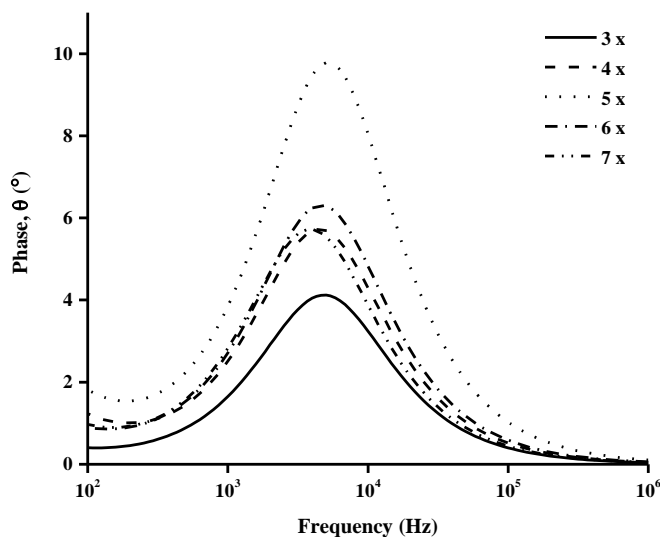


Figure 8. Bode plots with different spin coating layers

Table 2. EIS parameters with different spin coating layers

Sample	R_b (Ω)	R_{ct1} (Ω)	τ (ms)
rGO	-	25.0	0.03
Pt	-	36.98	0.01
3	65.35	22.75	0.20
4	64.68	14.37	0.22
5	64.70	17.89	0.20
6	64.67	24.74	0.22
7	64.65	22.78	0.25

4. CONCLUSIONS

Ag-rGO composites films were successfully prepared via layer-by-layer spin coating method and employed as cathode in DSSC. The device with 3 spin-coating cycles possesses the highest transmittance that is 7.5%. The device with 4 spin-coating cycles performed the highest η of 0.840% due to the smallest R_{ct} .

ACKNOWLEDGMENTS

This work was funded by Universiti Kebangsaan Malaysia (UKM) under research grant GUP-2018-081.

References

1. S. Yun, A. Hagfeldt, T. Ma, *ChemCatChem.*, 6, (2014) 1584.
2. Z. Huang, X. Liu, K. Li, D. Li, Y. Luo, H. Li, W. Song, L. Chen, Q. Meng, *Electrochem. Commun.*, 9 (2007) 596.
3. H. Zhu, H. Zeng, V. Subramanian, C. Masarapu, K.H. Hung, B. Wei, *Nanotech.*, 19 (2008) 465204.
4. J.G. Nam, Y.J. Park, B.S. Kim, J.S. Lee, *Scripta Mater.*, 62 (2010) 148.
5. M. Gulen, A. Sarilmaz, I.H. Patir, F. Ozel, S. Sonmezoglu, *Electrochim. Acta*, 269 (2018) 119.
6. R. Tas, M. Can, S. Sonmezoglu, *IEEE J. Photovolt.*, 7 (2017) 792.
7. F. Özel, A. Sarilmaz, B. İstanbullu, A. Aljabour, M. Kuş, S. Sonmezoglu, *Sci. Rep.*, 6 (2016) 29207.
8. R. Taş, M. Gülen, M. Can, S. Sönmezoğlu, *Synt. Met.*, 212 (2016) 75.
9. J.D. Roy-Mayhew, D.J. Bozym, C. Punckt, I.A. Aksay, *ACS Nano*, 4 (2010) 6203.
10. D.W. Zhang, X.D. Li, H.B. Li, S., Chen, Z. Sun, X.J. Yin, S.M. Huang, *Carbon*, 49 (2011) 5382.
11. H. Wang, K. Sun, F. Tao, D.J. Stacchiola, Y.H. Hu, *Angew. Chem. Int. Ed.*, 52 (2013) 9210.
12. L. Kavan, P. Liska, S.M. Zakeeruddin, M. Grätzel, *Electrochim. Acta*, 195 (2016) 34.
13. M.Y.A. Rahman, A.S. Sulaiman, A.A. Umar, M.M. Salleh, *J. Mater. Sci.: Mater. Electron.*, 28 (2017) 1674.
14. M.Y.A. Rahman, A.S. Sulaiman, A.A. Umar, *J. New Mater. Electrochem. Syst.*, 21 (2018) 113.
15. Z. Wang, P. Li, Y. Chen, J. He, J. Liu, W. Zhang, Y. Li, *J. Power Sources*, 263 (2014) 246.
16. Z. Wang, Y. Chen, P. Li, J. He, W. Zhang, Z. Guo, Y. Li, M. Dong, *RSC Adv.*, 6 (2016) 15080.
17. L. Wei, P. Wang, Y. Yang, R. Luo, J. Li, X. Gu, Z. Zhan, Y. Dong, W. Song, R. Fan, *J. Nanopart. Res.*, 20 (2018) 110.
18. M.I.A. Umar, C.C. Yap, R. Awang, A.A. Umar, M.M. Salleh, M. Yahaya, *Mater. Lett.*, 106 (2016) 200.
19. A.A. Umar, M.Y.A. Rahman, S.K.M. Saad, M.M. Salleh, M. Oyama, *Appl. Surf. Sci.*, 270 (2013) 109.
20. N. Mustaffa, M.Y.A. Rahman, A.A. Umar, *Arab. J. Chem.*, 13 (2019) 3383.
21. S. Akın, M. Gülen, S. Sayın, H. Azak, H.B. Yıldız, S. Sönmezoğlu, *J. Power Sources*, 307 (2016) 796.
22. S. Akın, S. Açıkgöz, M. Gülen, C. Akyürek, S. Sönmezoğlu, *RSC Adv.* 6 (2016) 85125.
23. A.Ö. Sönmezoğlu, S. Akın, B. Terzi, S. Mutlu, S. Sönmezoğlu, *Adv. Funct. Mater.*, 26 (2016) 8776.
24. S. Akin, E. Erol, S. Sonmezoglu, *Electrochim. Acta*, 225 (2017) 243.
25. T. Ozturk, B. Gulveren, M. Gulen, E. Akman, S. Sonmezoglu, *Solar Energy* 157 (2017) 47.
26. N. Mustaffa, M.Y.A. Rahman, A.A. Umar, *Ionics*, 24 (2018) 3665.

27. S.A. Salleh, M.Y.A. Rahman, Z. Yumni and T.H.T. Aziz, *Arab. J. Chem.*, 13 (2020) 5191.

28. U.A. Kamarulzaman, M.Y.A. Rahman, M.S. Su'ait and A.A. Umar, *J. Molecular Liquids*, 326 (2021) 115289.

© 2021 The Authors. Published by ESG (www.electrochemsci.org). This article is an open access article distributed under the terms and conditions of the Creative Commons Attribution license (<http://creativecommons.org/licenses/by/4.0/>)